

A metal mixture induces transformation upon antioxidant depletion in a hepatic cell line

Vicente Sánchez-Valle,* Mahara Valverde,* Leticia Carrizales,** Jesus Mejía,** Nahum Zepeta,* Emilio Rojas*

* Departamento de Medicina Genómica y Toxicología Ambiental, Instituto de Investigaciones Biomédicas, Universidad Nacional Autónoma de México, Ciudad de México, México.

** Facultad de Medicina, Universidad Autónoma de San Luis Potosí, San Luis Potosí, México.

ABSTRACT

Introduction. Metals are ubiquitous soil, air, and water pollutants. A mixture of arsenic cadmium and lead, in particular, has commonly been found in the vicinity of smelter areas. The mixture of As-Cd-Pb has been shown to be carcinogenic, and transforming potential and oxidative stress have been proposed as principal mechanisms involved in this process. The aim of this work was to explore the role of the antioxidant barrier in the establishment of cell transformation upon chronic exposure to a metal mixture containing 2 μM NaAsO₂, 2 μM CdCl₂, and 5 μM Pb(C₂H₃O₂)₂·3H₂O in WRL-68 cells-a non-transformed human hepatic cell line. **Material and methods.** In this study, we used a WRL-68 cell model of human embryonic hepatic origin treated with antioxidant inhibitors (L-Buthionine-sulfoxamine and aminotriazole) to test the role of the antioxidant barrier in the establishment of cell transformation upon chronic exposure to a metal mixture of As-Cd-Pb (2 μM NaAsO₂, 2 μM CdCl₂ and 5 μM Pb(C₂H₃O₂)₂·3H₂O). We evaluated oxidative damage markers, including reactive oxygen species, lipid peroxidation, and genotoxicity, as well as antioxidant response markers, including glutathione concentration, catalase activity, and superoxide dismutase activity, which promote morphological transformation, which can be quantified by foci formation. **Results.** As expected, we found an increase in the intracellular concentration of the metals after treatment with the metal mixture. In addition, treatment with the metal mixture in addition to inhibitors resulted in a large increase in the intracellular concentration of cadmium and lead. Our results describe the generation of reactive oxygen species, cytotoxicity, genotoxicity, and oxidative damage to macromolecules that occurred exclusively in cells that were morphologically transformed upon exposure to a metal mixture and antioxidant barrier inhibition. **Conclusion.** Our results show the importance of the antioxidant barrier role in the protection of cellular integrity and the transformation potential of this metal mixture via free radicals.

Key words. Arsenic. Cadmium. Lead. Morphological transformation. Aminotriazole. BSO. Antioxidant barrier. WRL68.

INTRODUCTION

Arsenic (As), cadmium (Cd) and lead (Pb) are ubiquitous air and water pollutants that continue to threaten the quality of public health around the world. Exposure to complex mixtures of metals in the workplace or environment is more likely to occur than exposure to a single metal alone.¹ These

three metals share several common mechanisms by which they exert their toxicities. In addition, stress proteins and antioxidant enzymes have been proposed to provide common protective cellular mechanisms against element-induced toxicities when they occur on an individual basis.² Furthermore, these metals have been included in the list of the top ten hazardous substances and are proposed as one of the mixtures for which interaction profile studies will be completed by the Agency for Toxic Substances and Disease Registry (ATSDR).³ As and Cd have been classified as carcinogens and Pb has been classified as a possible carcinogen by the International Agency in Research of Cancer (IARC).⁴

Metals are associated with a multitude of adverse health effects, such as cancer, hepatotoxicity, nephrotoxicity, and neurotoxicity.⁵ Some

Correspondence and reprint request: Emilio Rojas, PH.D.
Instituto de Investigaciones Biomédicas, Universidad Nacional Autónoma de México.
C.P. 04510, Ciudad de México, México.
E-mail: emilior@servidor.unam.mx

Manuscript received: April 23, 2012.
Manuscript accepted: September 20, 2012.

potential mechanisms involve the direct interaction of the metal with DNA or modification of DNA repair, DNA methylation status, and metabolic processes involved in DNA replication and expression.⁶⁻¹²

However, as a result of recent studies from a number of laboratories, oxidative stress is thought to play a major role in the development of As, Cd and Pb-related adverse health effects.^{2,13,14}

As, Cd and Pb generate reactive oxygen species (ROS) in the form of superoxide ($O_2^{\cdot-}$), singlet oxygen (1O_2), the peroxy radical (ROO^{\cdot}), nitric oxide (NO^{\cdot}), hydrogen peroxide (H_2O_2), the dimethylarsinic peroxy radical ($[(CH_3)_2AsOO^{\cdot}]$) and the dimethylarsinic radical $[(CH_3)_2As^{\cdot}]$.^{15,16} In addition, Cd treatment can cause iron replacement in some enzymes, and the accumulation of iron molecules reacts with H_2O_2 to produce hydroxyl radicals (HO^{\cdot}).^{16,17} ROS-generating mechanism of Pb is mediated by delta-aminolevulinic acid dehydratase (δ -ALAD) inhibition, which provokes the accumulation of delta-aminolevulinic acid (δ -ALA).^{16,18}

Defense against xenobiotic toxicity, which is composed of many types of antioxidants, is well characterized in mammals.^{19,20} We report here our study of the role of oxidative damage (and its modulation) in events evoked by the As-Cd-Pb metal mixture, in which we analyze the involvement of two preventive antioxidant compounds (catalase and glutathione) and their inhibitors in the modulation of the transformation process.

The hepatic cell line WRL-68 is a non-transformed human embryonic cell line that presents a morphological structure that is similar to hepatocytes and hepatic primary cultures. Derived from the fetal liver, WRL-68 preserves the activity of several characteristic liver enzymes and antioxidant efficient, providing an *in vitro* model to study the toxic effects of xenobiotics.²¹

In a previous report, using a two-step cell transformation model exposed to this metal mixture, we found an increase in the level of damage markers and the antioxidant response, a loss of cell viability and an elevation in the transforming potential. Cotreatment with N-acetyl-cysteine reduces the transforming capacity, suggesting the participation of oxidative stress in the transformation process.²² The aim of this work was to explore the role of the antioxidant barrier in the establishment of cell transformation upon chronic exposure to a metal mixture containing $2 \mu M$ $NaAsO_2$, $2 \mu M$ $CdCl_2$, and $5 \mu M$ $Pb(C_2H_3O_2)_2 \cdot 3H_2O$ in WRL-68 cells-a non-transformed human hepatic cell line.

MATERIAL AND METHODS

Chemical reagents

Dulbecco's modified Eagle's medium (D-MEM), antibiotic/antimicrobial, MEM, non-essential amino acids, and fetal bovine serum were obtained from Gibco-Mexico. Sodium m-arsenite, L-buthionine-sulfoxamine (BSO), 3-amino-1,2,4-triazole (3-ATZ), 2-thiobarbituric acid, O-phthalaldehyde (OPT), ethidium bromide (Et-Br), fluorescein diacetate (FDA), rhodamine-123, xanthine, xanthine oxidase, EDTA, nitro blue tetrazolium (NBT), sodium carbonate (Na_2CO_3), cupric chloride ($CuCl_2 \cdot 2H_2O$), normal agarose, and low melting point agarose were purchased from Sigma-Aldrich (St. Louis, MO, USA). Cadmium chloride was purchased from Mallinckrodt-Paris, lead acetate was from J.T Baker-Mexico, hydrogen peroxide (H_2O_2) was from Merck-Mexico, and bovine serum albumin was from USB Corporation-USA.

Cells, culture conditions, and exposure to the As, Cd, Pb mixture

WRL-68 is a non-transformed human hepatic cell line that is derived from the fetal liver and has a morphological structure that is similar to hepatocytes.

Cells were grown and maintained in Dulbecco's modified Eagle's medium supplemented with 10% fetal bovine serum, 1% non-essential amino acids, 100 U/mL penicillin and 100 $\mu g/mL$ streptomycin. Cells were incubated at $37^\circ C$ and 5% CO_2 . Approximately 5×10^4 cells/plaque were plated in 6-well culture plates and cultured reach to 80% confluency.

Four experimental groups were evaluated: an untreated group, a control group (C), which was cultivated as described above but with replacement of the maintenance medium every 72 h; a group (M) treated with the metal mixture ($2 \mu M$ $NaAsO_2$, $2 \mu M$ $CdCl_2$ and $5 \mu M$ $Pb(C_2H_3O_2)_2 \cdot 3H_2O$) every 72 h at a concentration that is equivalent to that for occupational exposure;^{23,24} a group (I) treated with a mixture of chemical inhibitors, including 1 mM L-buthionine-S,R-sulphoximine (BSO) (inhibitor of GSH synthesis), and 1.66 mM 3-aminotriazole (ATZ) (catalase inhibitor), which was applied for 2 h and repeated every 72 h; and a group (M + I) treated with the metal mixture and the mixture of antioxidant inhibitors every 72 h. Subcultures were treated every 5 days for 25 days of total treatment.

Measurement of the intracellular concentration of As, Cd, Pb

The intracellular quantification of metals was determined by atomic absorption spectrophotometry. For As, the samples were digested and analyzed using the hydride evolution technique with a Perkin-Elmer 3110 atomic absorption spectrometer.²⁵ Cd and Pb levels were determined using graphite furnace analyses with a Perkin-Elmer 2380 atomic absorption spectrophotometer. These methods detect the total metal concentration in the sample.

Cell viability

Cell viability was measured using the metabolic dual stain FDA method, as described by Hartmann and Speit.²⁶ Briefly, cells were mixed with a fluorochrome solution containing 0.02 $\mu\text{g}/\mu\text{L}$ Et-Br and 0.015 $\mu\text{g}/\mu\text{L}$ of FDA. The cells were then analyzed under a fluorescence microscope (Olympus BMX-60 with a UM61002 filter). Dead cells appeared red in color, and live ones appeared green. One hundred randomly chosen cells per condition were evaluated, and the results are expressed as percentages. All of the experiments were conducted in triplicate.

Detection of reactive oxygen species

This technique is based on the oxidation of dihydrorhodamine-123 to rhodamine-123 by reactive oxygen species.²⁷ Briefly, aliquots of 100 μL of the harvested samples (approximately 1×10^6 cells) were centrifuged at 1,200 rpm for 5 min. Next, the supernatant was poured off, and 180 μL of buffer A (140 mM NaCl, 5 mM KCl, 0.8 mM $\text{MgSO}_4 \cdot 7\text{H}_2\text{O}$, 1.8 mM CaCl_2 , 5 mM glucose, 15 mM HEPES) and 20 μL of dihydrorhodamine-123 (1 mM) were added. The samples were placed in a 96-well plate and read in a microplate reader (Biorad) at 505 nm. The results were interpolated from a standard curve of 0-10 μM rhodamine-123 in buffer A.

Determination of catalase activity

Catalase activity was measured according to the protocol described by Aebi.²⁸ Briefly, cells (approximately 1×10^6 cells) were washed two or three times with sterile PBS containing protease inhibitors. The cells were sonicated for 10 cycles of 10 seconds at an amplitude of 20 MHz. After sonication, the cells were centrifuged at 10,000 rpm for 5 min at 4 °C. The supernatant was used to determine the catalase

activity and protein concentration. The catalase activity was determined by reading the absorbance at 240 nm at room temperature, adjusting to zero with 50 mM phosphate buffer. H_2O_2 (500 μL of 20 mM) was added to 100 μL of supernatant and 400 μL of 50 mM phosphate buffer, and the absorbance was measured at 15 seconds and 30 seconds.

Determination of superoxide dismutase activity

Superoxide dismutase activity was measured following the protocol described by Sun, *et al.*²⁹ This method is based on the competition between superoxide dismutase and tetrazolium blue for the superoxide radicals formed by the xanthine oxidase system. The cells were sonicated and centrifuged at 10,000 rpm for 10 min at 4°C. Then, 200 μL of the supernatant was divided into two tubes with 1.85 mL of reaction mix (0.265 mM xanthine, 0.53 mM EDTA, 0.1325 mM NBT, 883 mg/mL albumin, 353 mM Na_2CO_3). To one tube, 50 μL of 50 mM phosphate buffer (blank) was added; to the other tube, 50 μL of 2-2.5 U/mL xanthine oxidase (sample) was added. These samples were incubated for 15 min. Next, 500 μL of CuCl_2 was added to quench the reaction. An aliquot of 200 μL of these samples was added to a 96-well microplate, and the absorbance was measured at 560 nm (A). The units of SOD were calculated as follows:

$$\text{Units of SOD} = \frac{[\text{A reaction mix} - (\text{A sample} - \text{A blank})]}{[\text{A reaction mix} (0.5\%)]}$$

Lipid peroxidation (Lpx)

The thiobarbituric acid method was used to measure the concentration of malondialdehyde (MDA).³⁰ A 100 μL aliquot (approximately 1×10^6 cells) was added to 100 μL of trichloroacetic acid (10% w/v) and centrifuged at 3,000 x g for 10 min. The supernatant was then added to 1 mL of thiobarbituric acid reagent (0.375%), and the mixture was heated at 92°C for 45 min. The absorbance of the thiobarbituric acid-MDA complex was measured at 532 nm using an ELISA spectrophotometer (Bio-Rad Model 550). Data were interpolated onto a concentration curve of 1,1,3,3-tetraethoxypropane ranging from 0 to 10 nM.

Comet assay

Ten microliters of the cell suspension ($1-1.5 \times 10^4$ cells) was mixed with 75 μL of a 0.5% LMP agarose

solution (0.36% final) and loaded onto microscope slides pre-layered with 150 μ L of 0.5% normal melting point agarose. The Comet assay was performed as described by Vega, *et al.*³¹ Briefly, after incubation with lysis buffer (2.5 M NaCl, 100 mM EDTA, 10 mM Tris, pH 10, supplemented with 10% DMSO and 1% Triton X-100) at 4°C for at least 1 h, the slides were placed in a horizontal electrophoresis chamber containing running buffer (300 mM NaOH, 1 mM EDTA, pH > 13). The slides remained in the electrophoresis buffer for 10 min to allow the DNA to unwind. Electrophoresis was performed for 10 min at 300 mA and 25 V (~ 0.8 V/cm), and all of the technical steps were conducted using very dim indirect light. After electrophoresis, the slides were gently removed and rinsed with neutralization buffer (0.4 M Tris, pH 7.5) at room temperature for 15 min. The slides were dehydrated with 100% ethanol for 15 min and air dried. Ethidium bromide (20 μ L of a 0.2 μ g/mL solution) was added to each slide, and a coverslip was placed on the gel. Individual cells were visualized at 20x magnification using an Olympus BX-60 microscope with fluorescence attachments (515-560 nm excitation filter, 590 nm barrier filter). Images were digitized and analyzed using KOMET v.31 software (Kinetic Imaging), and the Olive tail moment (OTM) parameter was used to evaluate DNA damage (200 cells were scored for each condition).

***In vitro* evaluation of cell transformation**

Cell transformation was evaluated according to the morphologic parameters of the IARC/NCI/EPA Working Group.³² Transformed foci were scored according to the following criteria, which discriminate these foci based on four morphological characteristics:

- Diameter > 2 mm.
- Deep basophilic staining.
- Dense multi-layering of cells, and
- Random orientation of cells at the edge of the foci.^{33,34}

Assay of anchorage-independent cell growth

The anchorage-independent growth of hepatocytes was monitored using the soft agar colony formation assay a selective test to evaluate the cell transformation capacity. Disaggregated cells (1×10^4) were plated in six-well plates containing 0.3% Noble agar in DMEM with 10% FBS and incubated

at 37°C and 5% CO₂. Colonies were evaluate after 14 days, fixed with 70% ethanol, and stained with Coomassie Blue.³⁵

Statistical analysis

Results are expressed as means \pm standard error (SE). The statistical significance between the experimental groups and the control group was calculated by analysis of variance (ANOVA) with Bonferroni correction, and post hoc analysis was performed between groups. P-values of < 0.05 were considered to be significant. All analyses were performed using the statistical software Sigma Stat (V).

RESULTS

Intracellular metal quantification and cellular viability in WRL-68 cells subjected to several treatments

The metals were present at a very low intracellular concentration in cells treated with the inhibitor mixture (group I) throughout the treatment period, similar to the control cells (group C) (Table 1). In contrast, cells treated with the metal mixture (group M) and the metal mixture plus inhibitors (group M + I) showed an increase in their intracellular metal concentration, with a significant accumulation of Pb in group M + I after 25 days of treatment (Table 1). Cell viability remained constant at over 90% in all groups during the 25 days of treatment, except at day 5 in group M+I, in which a loss in cell viability was observed, representing clonal selection of cells exposed to this treatment and suggesting an initiation phase for the cell transformation process (Table 1).

Chemical inhibition of antioxidants

We observed a decrease in the concentration of GSH in group I and an increase in GSH in group M as compared to group C (Figure 1A). The percentage of SOD activity for the experimental groups had a similar trend to that for group C until day 15; a significant increase was induced by all treatments on day 25, and this increase was exacerbated in group M + I (Figure 1B). The percentage of CAT activity was constantly inhibited by all treatments during the first 15 days and reached a similar activity to that of group C after 25 days (Figure 1C).

Table 1. Viability of WRL-68 cells treated for 25 days, measured by the dual stain FDA method, and the intracellular quantification of metals, measured by atomic absorption spectrophotometry.

Days	Treatment	Viability (%)	As (µg/L)	Cd (µg/L)	Pb (µg/L)
5	C	100 ± 2.8	0.526 ± 0.020	3.359 ± 0.001	4.287 ± 0.760
	M	100 ± 0	9.805 ± 0.059**	4.298 ± 0.000**	37.475 ± 6.031**
	I	98 ± 2.8	1.276 ± 0.022**	3.317 ± 0.000*	5.475 ± 0.700
	M + I	23 ± 0**	21.07 ± 0.078**	7.549 ± 0.001**	22.955 ± 0.021**
15	C	100 ± 0	1.203 ± 0.020	6.441 ± 0.001	4.972 ± 1.460
	M	100 ± 1.4	14.316 ± 0.130**	10.217 ± 0.014**	31.35 ± 4.228**
	I	96 ± 2.8*	0.667 ± 0.029**	2.739 ± 0.002**	5.94 ± 2.291
	M + I	100 ± 0	11.863 ± 0.453**	10.107 ± 0.014**	98.815 ± 3.500**
25	C	100 ± 1.4	0.508 ± 0.007	4.794 ± 0.001	5.4 ± 2.206
	M	97 ± 0*	11.413 ± 0.130**	5.67 ± 0.001**	44.64 ± 5.798**
	I	91 ± 2.1*	0.403 ± 0.019**	2.241 ± 0.001**	4.55 ± 1.258
	M + I	100 ± 0.7	14.513 ± 0.030**	12.617 ± 0.014**	117.515 ± 0.035**

C: control. M: metal mixture. I: inhibitor mixture. M + I: metal mixture plus inhibitor mixture. All results represent the average of three independent experiments. *p < 0.05, **p < 0.005. ANOVA and *post hoc* analysis with respect to the control condition.

Evaluation of reactive oxygen species and molecular target effects

We observed an increase in the ROS concentration on days 15 and 25 in group M + I, while the remaining groups did not show an induction of ROS (Figure 2A). Lipid peroxidation significantly increased in group M + I on days 15 and 25 (Figure 2B). DNA strand breaks, assessed using the alkaline comet assay, were induced in group M + I at all treatment times (Figure 2C). It is worth noting that we also observed DNA damage in group M at 5 and 25 days of treatment.

Induction of cell transformation

Cell transformation was observed as morphological changes in group M + I. We observed the formation of foci from day 15 of culture using Giemsa staining, with a mean of 84 ± 21.58 foci per flask. However, we did not observe the formation of any foci in groups C, M, or I (Figure 3A and 3B). To confirm the morphological transformation state, the cells were cultured in soft agar, and the cells treated with M + I were able to grow under this condition (Figure 3C).

DISCUSSION

Mixtures of metals, such as As, Cd and Pb, are widely distributed in the environment as a result of human activities. These three elements are among the top ten substances in the priority list

of hazardous substances of the Superfund of the United States.³⁶ In most cases, these metals exist together and are among the first binary combinations of contaminants in soil and water.³⁷ Therefore, most human populations are chronically exposed to these elements as a mixture. Accordingly, it is important to investigate the possible mechanisms of carcinogenicity of the As-Cd-Pb mixture as well as the participation of antioxidant molecules in the process of cell transformation associated with exposure to this mixture. Currently, these mechanisms are not fully understood.

After the treatment of cells with the As-Cd-Pb mixture, we observed an increase in the intracellular concentration of these metals in group M, while in group M + I, we observed a large increase in the concentration of intracellular Pb compared to group M. This effect has been reported previously;³⁸ however, there are different theories to explain it. Kowaltowski, *et al.*³⁹ showed that 3-aminotriazole inhibits catalase and metallothionein and activates some Pb and Cd protein transporters as a result of the increase in metal absorption. However, Doroshenko and Doroshenko⁴⁰ and Lee, *et al.*⁴¹ proposed an increase in calcium influx that is dependent on L-type Ca^{2+} channels and induced by oxidative stress due to GSH depletion. Additionally, Hinkle, *et al.*⁴² and Lou, *et al.*⁴³ discussed the activity of calcium transporters and anion exchangers when metal absorption is increased. Further studies are needed to clarify which of these mechanisms is responsible for the intracellular increase in Pb in the presence of antioxidant inhibitors.

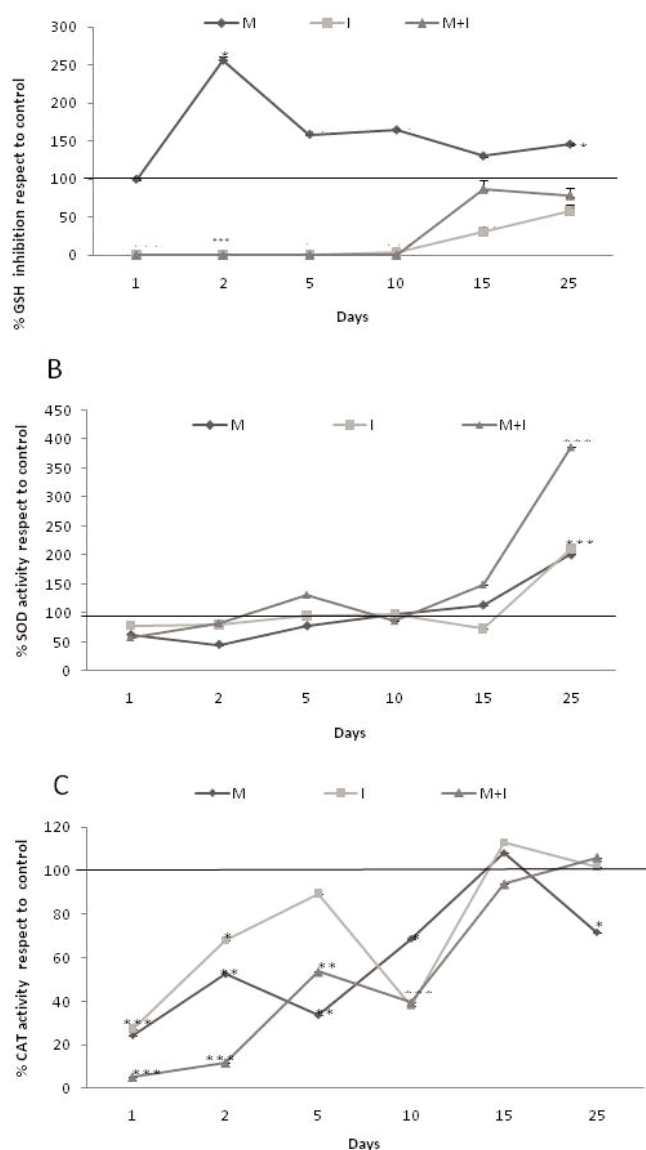


Figure 1. Activity of antioxidants. **A.** GSH concentration, detected using the OPT method. **B.** SOD activity, evaluated using the xanthine oxidase system. **C.** CAT activity, determined via the degradation of H_2O_2 . The horizontal line on the Y axis represents the relative value of the control group (100%) compared to the other groups. M: Metal mixture. I: inhibitor mixture. M + I: metal mixture plus inhibitor mixture. All results represent the average of three independent experiments. * $p < 0.05$, ** $p < 0.005$. ANOVA and post hoc analysis with respect to the control condition.

An imbalance between oxidants and antioxidants, which can cause oxidative stress, is thought to underlie metal carcinogenicity.¹⁶ Increasing evidence exists for the attenuation of individual antioxidant defense mechanisms during tumor development. Reiners, *et al.*⁴⁴ reported a significant decrease in SOD,

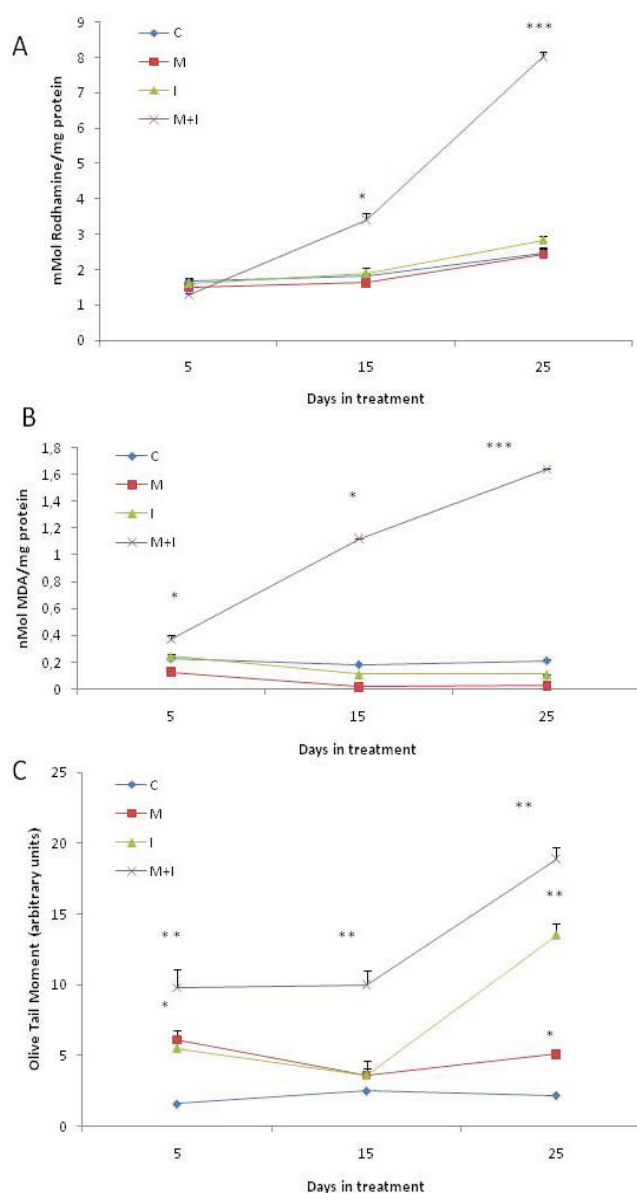


Figure 2. Reactive oxygen species and molecular targets of oxidation. **A.** Reactive oxygen species (ROS), measured by the oxidation of dihydrorhodamine-123. **B.** Lipid peroxidation (LPX), measured using the T-BARS reaction. **C.** DNA damage, determined as single strand breaks with the Comet assay. All results represent the average of three independent experiments. * $p < 0.05$, ** $p < 0.005$. ANOVA and post hoc analysis with respect to the control condition.

catalase and glutathione peroxidase activities in SENCAR mouse skin following exposure to TPA. The specific activities of SOD and catalase in papillomas and carcinomas generated using an initiation-promotion protocol were also found to be similarly depressed compared to those in normal skin.

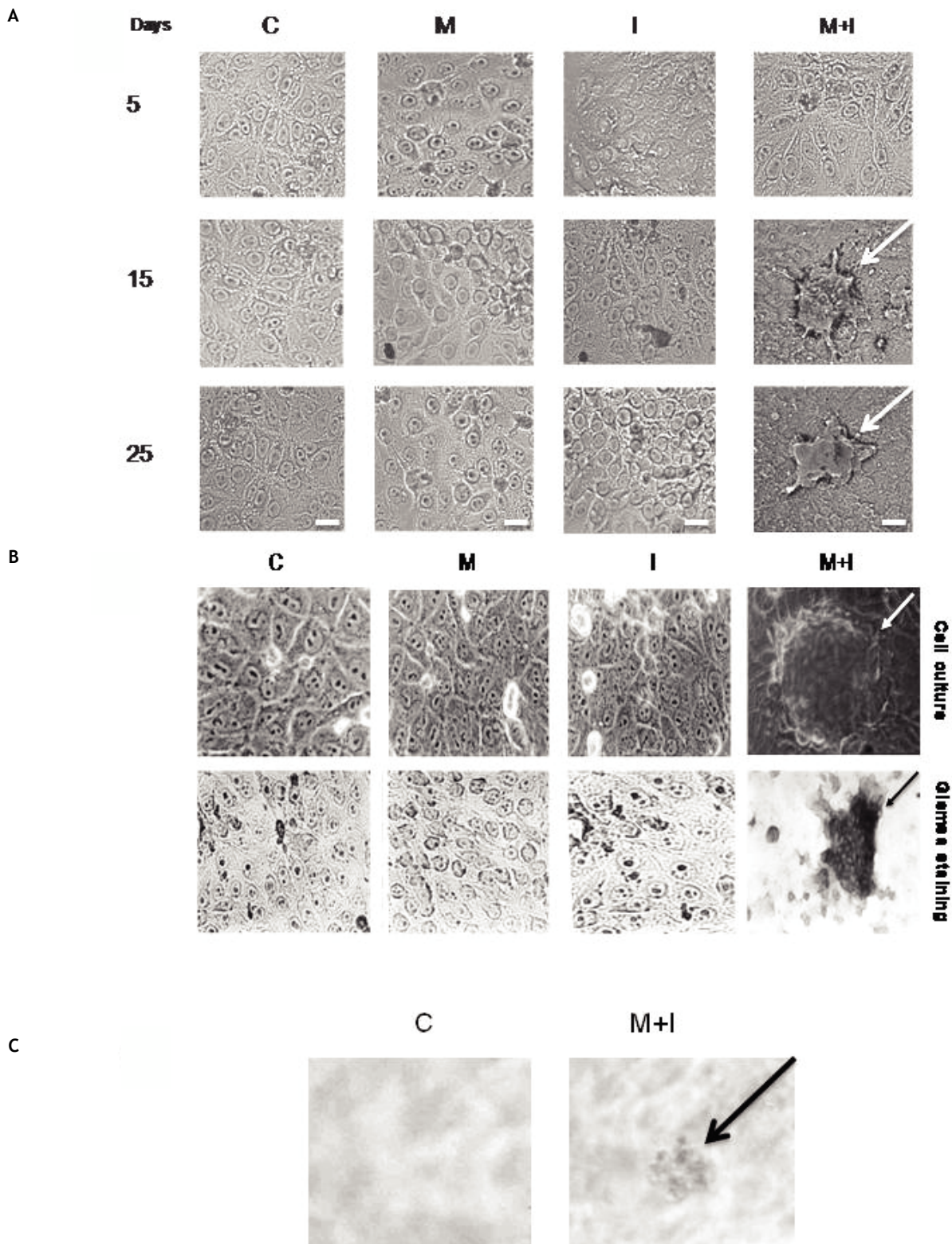


Figure 3. Cellular transformation characteristics of WRL-68 cells treated for 25 days in culture, observed by light microscopy at 40X. **A.** Morphology of cells exposed to different treatments for 25 days. **B.** Transformed foci with intense basophilia, assessed by Giemsa staining. **C.** Positive cell transformation test for anchorage-independent in soft agar. C: Control. M: Metal mixture. I: inhibitor mixture. M + I: metal mixture plus inhibitor mixture. Bars = 10 μ m.

Furthermore, the promotion and progression of skin tumors in different strains of mice were shown to correlate with oxidative events and DNA damage.⁴⁵

Data in the literature suggest that the modulation of catalase activity may be mechanistically involved in the deregulation of signaling cascades during tumor promotion-progression, with pathways regulated by the trans-activation of AP-1, NF- κ B and CREB being significantly impacted.⁴⁶

However, the attenuation of GSH generates oxidative stress and subsequently leads to the induction of JNK/SAPK and p38 MAPK, which are necessary components of the cellular defense program against cytotoxic xenobiotics.⁴⁷ Therefore, it is possible that a sustained reduction in glutathione levels facilitated the emergence of a xenobiotic-resistant, malignantly transformed phenotype upon repeated treatments with xenobiotic agent. An interesting observation was the increase GSH concentration upon metal treatment. This result is paradoxical because the GSH content should decrease following exposure to pro-oxidant metals due to consumption. However, many studies have focused on the transcriptional regulation of enzymes to synthesize GSH. NF κ B, Sp-1, AP-1, activator protein-2 (AP-2), metal response elements (MRE), and antioxidant response elements (ARE) have been identified in the human gamma-glutamyl cysteine ligase (GCL) promoter. Many studies have identified a proximal AP-1 element (-263 to -269) as a critical mediator of the oxidative stress-induced increase in human GCL transcription. Moreover, the activation of the ARE pathway could explain why xenobiotics cause an increase in the GSH concentration as a first response.^{48,49}

In addition to the diminution in antioxidant levels, ROS, lipid peroxidation and genotoxicity were consistently found in cells treated with both metals and inhibitors over time. Considering that DNA damage was present during all treatment times (Figure 2C), we suggest that the DNA repair system may have been impaired by the metal mixture treatment, in addition to the observed genotoxicity; these effects have also been observed in other studies.^{11,50} An increase in oxidative stress markers, such as ROS and lipid peroxidation, were observed uniformly over time in cells treated with both metals and inhibitors (Figure 2). Inactivating the antioxidant machinery with 3-AT and BSO may resulted in increased levels of ROS in metal-treated cells and, subsequently, enhanced lipid peroxidation and genotoxicity. The enhancing effect of 3-AT on genotoxicity induced by exposure to cadmium at low concentrations (1-2 μ M) has

been suggested to be partially due to a higher intra-cellular concentration of cadmium as a result of 3-ATZ; however, the authors did not observe the same pattern when performing the same experiments with lead.⁴⁶

In this scenario, the M+I treated cells presented morphological alterations; they lost their hepatic cell characteristics. It is worth noting that cells chronically treated with the metal mixture at nanomolar concentrations for more than 4 months did not show any morphological changes (data not shown). To determine whether the morphological changes induced by exposure to the metal mixture were related to transformation, we evaluated the capacity of these cells to grow in anchorage-independent conditions. Anchorage independence is believed to be one step in the multi-step process of the neoplastic transformation of human fibroblasts, and it has proven to be a particularly attractive endpoint for transformation studies;³⁸ however, the biochemical changes of cells with anchorage-independent phenotypes are not yet fully understood. Several studies have suggested that anchorage independence results from a mutational or epigenetic event because the acquired anchorage-independent phenotype is a permanent characteristic of the cells.^{51,52} Moreover, some reports link the use of antioxidant inhibitors with an enhancement of anchorage independence. For instance, 3-ATZ has been reported to significantly enhance cadmium-induced anchorage independence and cytotoxicity in diploid human fibroblasts HFW, thus supporting the notion that ROS is involved in cadmium genotoxicity;^{38,53} this increase in metal uptake by 3-ATZ does not occur at high cadmium-treatment doses (10 mM). In contrast, 3-ATZ neither affects lead-induced anchorage independence and cytotoxicity nor induces the weak mutagenicity of lead, even though 3-ATZ does enhance lead uptake and accumulation in HFW cells.

CONCLUSION

In our study, we established a model that is sensitive to cell transformation using human cells, which could be useful tool for the study of chemical carcinogenesis. Moreover, in this model we showed the cell transforming effect of metal mixture (As-Cd-Pb) at concentrations equivalent to those reported for occupationally exposed individuals. We also demonstrated that the balance between the antioxidant status and oxidant insult generated by the mixture of metals plays a pivotal role in the process

of cell transformation. In general our findings could provide new insights in the field such as the use of different antioxidant parameters as a risk associated biomarkers and interventional design studies of the population exposed to these metals.

ACKNOWLEDGEMENTS

We are grateful to all of the cooperating organizations that made this study possible: Universidad Nacional Autónoma de México, Doctorado en Ciencias Biomédicas and Consejo Nacional de Ciencia y Tecnología M47330.

REFERENCES

- Carrizales L, Razo I, Tellez-Hernandez JI, Torres-Nerio R, Torres A, Batres LE, Cubillas AC, et al. Exposure to arsenic and lead of children living near a copper-smelter in San Luis Potosi, Mexico: Importance of soil contamination for exposure of children. *Environ Res* 2006; 101: 1-10.
- Wang G, Fowler BA. Roles of biomarkers in evaluating interactions among mixtures of lead, cadmium and arsenic. *Toxicol Appl Pharmacol* 2008; 233: 92-9.
- ATSDR (Agency for Toxic Substances and Disease Registry). 2007. Primary known toxic pollutants list from and possible technology advances to harness, sequester or fix the air and water pollution caused by them-new technologies and possible solutions.
- IARC 2006. Monographs on the Evaluation of Carcinogenic Risks to Humans. Inorganic and Organic Lead Compounds. Vol. 87.
- Madden EF, Fowler BA. Mechanisms of nephrotoxicity from metal combinations: a review. *Drug Chem Toxicol* 2000; 23: 1-12.
- Banerjee S, Flores-Rozas H. Cadmium inhibits mismatch repair by blocking the ATPase activity of the MSH2-MSH6 complex. *Nucleic Acids Res* 2005; 33: 1410-9.
- Clark AB, Kuntel TA. Cadmium inhibits the functions of eukaryotic MutS complex. *J Biol Chem* 2004; 279: 52903-6.
- Giaginis C, Gatzidou E, Theocharis S. DNA repair systems as targets of cadmium toxicity. *Toxicol Appl Pharmacol* 2006; 213: 282-90.
- Kopera E, Schwerdtle T, Hartwig A, Bal W. Co(II) and Cd(II) substitute for Zn(II) in the zinc finger derived from the DNA repair protein XPA, demonstrating a variety of potential mechanisms of toxicity. *Chem Res Toxicol* 2004; 17: 1452-8.
- Leonard SS, Harris GK, Shi X. Metal-induced oxidative stress and signal transduction. *Free Radic Biol Med* 2004; 37: 1921-42.
- McNeill DR, Narayana A, Wong HK, Wilson DM 3rd. Inhibition of Ape1 nuclease activity by lead, iron, and cadmium. *Environ Health Perspect* 2004; 112: 799-804.
- Witkiewicz-Kucharczyk A, Bal W. Damage of zinc fingers in DNA repair proteins, a novel molecular mechanism in carcinogenesis. *Toxicol Lett* 2006; 162: 29-42.
- Del Carmen EM, Souza V, Bucio L, Hernández E, Damián-Matsumura P, Zaga V, Gutiérrez-Ruiz MC. Cadmium induces alpha(1)collagen (I) and metallothionein II gene and alters the antioxidant system in rat hepatic stellate cells. *Toxicology* 2002; 170: 63-73.
- Valverde M, Trejo C, Rojas E. Is the capacity of lead acetate and cadmium chloride to induce genotoxic damage due to direct DNA-metal interaction? *Mutagenesis* 2001; 16: 265-70.
- Cooper KL, Liu KJ, Hudson LG. Enhanced ROS production and redox signaling with combined arsenite and UVA exposure: contribution of NADPH oxidase. *Free Radic Biol Med* 2009; 47: 381-8.
- Valko M, Rhodes CJ, Moncol J, Izakovic M, Mazur M. Free radicals, metals and antioxidants in oxidative stress-induced cancer. *Chem Biol Interact* 2006; 160: 1-40.
- Liu J, Qu W, Kadiiska MB. Role of oxidative stress in cadmium toxicity and carcinogenesis. *Toxicol Appl Pharmacol* 2009; 238: 209-14.
- Ahamed M, Singh S, Behari JR, Kumar A, Siddiqui MK. Interaction of lead with some essential trace metals in the blood of anemic children from Lucknow, India. *Clin Chim Acta* 2007; 377: 92-7.
- Noguchi N, Watanabe A, Shi H. Diverse functions of antioxidants. *Free Radic Res* 2000; 33: 809-17.
- Cicchetti R, Argentin G. The role of oxidative stress in the in vitro induction of micronuclei by pesticides in mouse lung fibroblasts. *Mutagenesis* 2003; 18: 127-32.
- Gutiérrez-Ruiz MC, Bucio L, Souza V, Gomez JJ, Campos C, Carabez A. Expression of some hepatocyte-like functional properties of WRL-68 cells in culture. *In Vitro Cell Dev Biol Anim* 1994; 30A: 366-71.
- Silva Aguilar M, Rojas E, Valverde M. Role of oxidative stress in transformation induced by metal mixture. *Oxid Med Cell Longev* 2011; 2011: 935160.
- Merzenich H, Hartwig A, Ahrens W, Beyersmann D, Schlegel R, Scholze M, Timm J, et al. Biomonitoring on carcinogenic metals and oxidative DNA damage in a cross-sectional study. *Cancer Epidemiol Biomarkers Prev* 2001; 10: 515-22.
- Palus J, Rydzynski K, Dziubaltowska E, Wyszynska K, Natarajan AT, Nilsson R. Genotoxic effects of occupational exposure to lead and cadmium. *Mutat Res* 2003; 540: 19-28.
- De la Fuente H, Portales-Perez D, Baranda L, Díaz-Barriga F, Saavedra-Alanis V, Layseca E, González-Amaro R. Effect of arsenic, cadmium and lead on the induction of apoptosis of normal human mononuclear cells. *Clin Exp Immunol* 2002; 129: 69-77.
- Hartmann A, Speit G. Genotoxic effects of chemicals in the single cell gel (SCG) test with human blood cells in relation to the induction of sister-chromatid exchanges (SCE). *Mutat Res* 1995; 346: 49-56.
- Lee VM, Quinn PA, Jennings SC, Ng LL. NADPH oxidase activity in preeclampsia with immortalized lymphoblasts used as models. *Hypertension* 2003; 41: 925-31.
- Aebi H. Catalase in vitro. *Methods Enzymol* 1984; 105: 121-6.
- Sun Y, Oberley LW, Li Y. A simple method for clinical assay of superoxide dismutase. *Clin Chem* 1988; 34: 497-500.
- Bouaicha N, Maatouk I. Microcystin-LR and nodularin induce intracellular glutathione alteration, reactive oxygen species production and lipid peroxidation in primary cultured rat hepatocytes. *Toxicol Lett* 2004; 148: 53-63.
- Vega L, Valverde M, Elizondo G, Leyva JF, Rojas E. Diethylthiophosphate and diethyldithiophosphate induce genotoxicity in hepatic cell lines when activated by further biotransformation via Cytochrome P450. *Mutat Res* 2009; 679: 39-43.
- IARC/NCI/EPA Working Group. Cellular and molecular mechanisms of cell transformation and standardization of

- transformation assays of established cell lines for the prediction of carcinogenic chemicals: overview and recommended protocols. *Cancer Res* 1985; 45: 2395-9.
33. Kajiwarra Y, Ajimi S. Verification of the BALB/c 3T3 cell transformation assay after improvement by using an ITES-medium. *Toxicol In Vitro* 2003; 17: 489-96.
 34. Tsuchiya T, Tanaka-Kagawa T, Jinno H, Tokunaga H, Sakimoto K, Ando M, Umeda M. Inorganic arsenic compounds and methylated metabolites induce morphological transformation in two-stage BALB/c 3T3 cell assay and inhibit metabolic cooperation in V79 cell assay. *Toxicol Sci* 2005; 84: 344-51.
 35. Yoo SM, Antonyak MA, Cerione RA. The adaptor protein and Arf GTPase-activating protein Cat-1/Git-1 is required for cellular transformation. *J Biol Chem* 2012; 37: 31462-70.
 36. De Rosa CT, Johnson BL, Fay M, Hansen H, Mumtaz MM. Public health implications of hazardous waste sites: findings, assessment and research. *Food Chem Toxicol* 1996; 34: 1131-8.
 37. Fay RM, Mumtaz MM. Development of a priority list of chemical mixtures occurring at 1188 hazardous waste sites, using the HazDat database. *Food Chem Toxicol* 1996; 34: 1163-5.
 38. Hwua YS, Yang JL. Effect of 3-aminotriazole on anchorage independence and mutagenicity in cadmium- and lead-treated diploid human fibroblasts. *Carcinogenesis* 1998; 19: 881-8.
 39. Kowaltowski AJ, Vercesi AE, Rhee SG, Netto LE. Catalases and thioredoxin peroxidase protect *Saccharomyces cerevisiae* against Ca(2+)-induced mitochondrial membrane permeabilization and cell death. *FEBS Lett* 2000; 473: 177-82.
 40. Doroshenko N, Doroshenko P. The glutathione reductase inhibitor carmustine induces an influx of Ca2+ in PC12 cells. *Eur J Pharmacol* 2004; 497: 17-24.
 41. Lee M, Cho T, Jantarantotai N, Wang YT, McGeer E, McGeer PL. Depletion of GSH in glial cells induces neurotoxicity: relevance to aging and degenerative neurological diseases. *FASEB J* 2010; 24: 2533-45.
 42. Hinkle PM, Shanshala ED 2nd, Nelson EJ. Measurement of intracellular cadmium with fluorescent dyes. Further evidence for the role of calcium channels in cadmium uptake. *J Biol Chem* 1992; 267: 25553-9.
 43. Lou M, Garay R, Alda JO. Cadmium uptake through the anion exchanger in human red blood cells. *J Physiol* 1991; 443: 123-36.
 44. Reiners JJ Jr, Thai G, Rupp T, Cantu AR. Assessment of the antioxidant/prooxidant status of murine skin following topical treatment with 12-O-tetradecanoylphorbol-13-acetate and throughout the ontogeny of skin cancer. Part I: Quantitation of superoxide dismutase, catalase, glutathione peroxidase and xanthine oxidase. *Carcinogenesis* 1991; 12: 2337-43.
 45. Wei L, Wei H, Frenkel K. Sensitivity to tumor promotion of SENCAR and C57BL/6J mice correlates with oxidative events and DNA damage. *Carcinogenesis* 1993; 14: 841-7.
 46. Gupta A, Butts B, Kwei KA, Dvorakova K, Stratton SP, Briehl MM, Bowden GT. Attenuation of catalase activity in the malignant phenotype plays a functional role in an in vitro model for tumor progression. *Cancer Lett* 2001; 173: 115-25.
 47. Wilhelm D, Bender K, Knebel A, Angel P. The level of intracellular glutathione is a key regulator for the induction of stress-activated signal transduction pathways including Jun N-terminal protein kinases and p38 kinase by alkylating agents. *Mol Cell Biol* 1997; 17: 4792-800.
 48. Lu SC. Regulation of glutathione synthesis. *Mol Aspects Med* 2009; 30: 42-59.
 49. Croute F, Beau B, Murat JC, Vincent C, Komatsu H, Obata F, Soleilhavoup JP. Expression of stress-related genes in a cadmium-resistant A549 human cell line. *J Toxicol Environ Health A* 2005; 68: 703-18.
 50. Hartwig A, Schwerdtle T. Interactions by carcinogenic metal compounds with DNA repair processes: toxicological implications. *Toxicol Lett* 2002; 127: 47-54.
 51. Kenney NJ, Saeki T, Gottardis M, Kim N, Garcia-Morales P, Martin MB, Normanno N, et al. Expression of transforming growth factor alpha antisense mRNA inhibits the estrogen-induced production of TGF alpha and estrogen-induced proliferation of estrogen-responsive human breast cancer cells. *J Cell Physiol* 1993; 156: 497-514.
 52. Ciardiello F, Pepe S, Bianco C, Baldassarre G, Ruggiero A, Bianco C, Selvam MP, et al. Down-regulation of RI alpha subunit of cAMP-dependent protein kinase induces growth inhibition of human mammary epithelial cells transformed by c-Ha-ras and c-erbB-2 proto-oncogenes. *Int J Cancer* 1993; 53: 438-43.
 53. Wiseman H, Halliwell B. Damage to DNA by reactive oxygen and nitrogen species: role in inflammatory disease and progression to cancer. *Biochem J* 1996; 313 (Pt. 1): 17-29.